Journal of Physics: Conference Series **2940** (2025) 012002 doi:10.1088/1742-6596/2940/1/012002

Accuracy in evaluating convective heat transfer coefficient by RANS CFD simulations in a rectangular channel with high aspect ratio and V-shaped ribs

M Corti[1], P Gramazio[1], D Fustinoni[1] and A Niro[1,*]

[1] Politecnico di Milano, Department of Energy via Lambruschini 4, 20156 Milano, Italy

E-mail: *alfonso.niro@polimi.it

Abstract. In the framework of heat transfer enhancement inside channels with ribbed surfaces, V-shaped ribs are placed as the most promising among the standard-shaped ribs. This works aims to present a numerical analysis of heat transfer characteristics for forced convection inside a rectangular channel with high aspect ratio 1:10 equipped with V-shaped ribs. CFD simulations are carried out by means of Reynolds Averaged Navier-Stokes (RANS) equations, working with an air flow inside a narrow rectangular channel 120 mm wide and 840 mm long. V-shaped ribs have square cross section and they have been tested both with the tip of the V pointing downwards both upwards with respect to the channel inlet. For each configuration three different values of dimensionless pitch (10, 20 and 40) have been analysed. Comparisons between numerical and experimental data on convective global heat transfer coefficient and pressure drops are presented, showing very good agreement. Finding a properly working CFD model is useful for authors because this work, together with previous studies on 90° and 60° ribs, aims to be exploited during parametric early design-phases of new heat exchangers.

Keywords: forced convection, heat exchanger, rectangular channel, ribbed surfaces, CFD validation

1. Introduction

Heat transfer enhancement is crucial in several industrial applications as well as in the transport sector. High performance heat exchangers are required for electronic components cooling especially associated to modern applications such as high performance CPUs cooling and electric motors or batteries cooling of electric vehicles [1] in addition to traditional applications like gas turbine and solar air heaters.

Analyzing the most recent reviews [2–4] in literature related to this broad field, it is possible to conclude that, as far as ribbed channels with conventional ribs are concerned, V-shaped and W-shaped ribs configurations are the most favourable for heat transfer enhancement. It has also been found that the optimum angle of attack is 60° for both configurations. Furthermore, heat transfer enhancement sees an increase if V-shaped ribs present gaps along them [5].

Over years, the authors have conducted many experimental measurements on heat transfer and fluid-dynamics regarding forced convection inside channel of high aspect ratio (AR) with ribs. We have tested conventional ribs varying pitch-to-side and blockage ratio, and all of these heat transfer and fluid-dynamic data have now been exploited for creating a reliable CFD model applicable for a wide range of ribs configurations that could be used as starting point for the early design phase of new heat exchangers. In this work we present a comparison between experimental and numerical results regarding high AR rectangular channel with 60° V-shaped ribs.

2. Model and method

2.1. Experimental setup

The experimental setup can be easily summarized as a rectangular channel with AR=10 in which air flows at Reynolds between 700 and 8000. The air encounters ribs on the upper and lower channel walls which operate at a constant temperature, while ribs are adiabatic as the lateral walls. In this specific case air flows at Reynolds number of 7200 and ribs are V-shaped with an angle of attack of 60° degree (with respect to the main stream). They have been called V_{down} and V_{up} depending on what is the direction the apexes of the ribs: V_{down} ribs have apexes pointing towards the flow direction, while V_{up} ribs have apexes pointing forward the flow direction. In this study ribs have a squared cross section with e = s = 4 mm, they are parallel and in line as can be seen in figure 1. Moreover, we have considered for both configuration three different adimensional pitch-to-side ratio (p/s): 10, 20, 40, namely P10S4, P20S4, P40S4. For further details and information on measurements, data processing and error analysis we suggest you refer to [6], while table 1 presents a summary of the geometric parameters.

2.2. Numerical procedure

The computational domain is a 3D rectangular channel made up of three different solids. These are merged to create a test section, an inlet region and an outlet region. This approach helps to mitigate issues associated with reverse flow, particularly common in geometries featuring internal turbulators. Air, treated as an incompressible fluid, is the working fluid and is operated at Reynolds 7200 providing a turbulent flow regime.

The air enters the domain at $T_{in} = 296K$ or $T_{in} = 300K$ depending on the configuration considered. The temperature profile develops along the channel while the velocity profile at the inlet is fully developed, obtained in previous simulations at the same Reynolds number in an identical channel but without ribs. At the outlet $P_{out} = 0$ is applied. Walls are subject to a no-slip velocity condition, all surfaces −upper, lower, and lateral− operated at constant temperature $T_{wall} = 313.15K$. This condition does not apply to ribs walls, they are all considered adiabatic, with $q = 0$ imposed. This distinction is made to emphasize the beneficial fluid-dynamic effects of the ribs, dissociating them from potential fin-like behaviors. Also in the experimental setup they

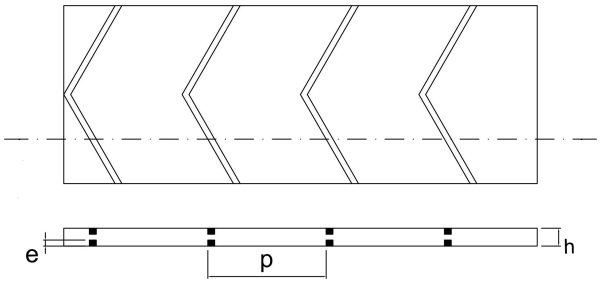

Figure 1. V_{up}, $\alpha = 60°$, in line.

Table 1. Channel geometric parameters.

	Value [m]
Height, h=H/2	0.012
Width, w=W/2	0.12
Length, L	0.84
Hydraulic diameter, Dh	0.02128
Ribs height, ribs width, e = s	0.004

have very low thermal conductivity, since they are made in wood and/or Plexiglass. For this work we applied symmetries along length and spanwise direction, managing to work with a quarter of the domain. The boundary conditions presented are consistent with the experimental setup, with the exception of the lateral walls. In the numerical setup they are considered at constant temperature, whereas in the experimental setup they are almost adiabatic. This difference is based on prior studies [7], which demonstrate that the heating of the lateral walls at constant temperature provides the most appropriate representation of the experimental configuration within the numerical framework.

Numerical simulations were performed exploiting the Ansys Fluent 2023 R1 software platform. The flow field is modelled using RANS, with the $k-\omega-$SST turbulence model. The SIMPLEC algorithm was chosen among the others after some comparative analysis from earlier tests, exhibiting better and quicker convergence. We carried out a sensitivity analysis to be sure of proposing a grid-independent solution, by examining variations along all three directions. Notably, we observed that the influence of the mesh is more significant along channel height (y). In summary, after testing structured grids with consistent topologies varying the number of elements, a grid with approximately $80 \cdot 10^6$ elements was selected for the entire channel, meaning approximately $20 \cdot 10^6$ elements for the considered computational domain, reduced thanks to symmetries, but the exact number of elements may vary depending on the specific channel configuration as the number of ribs varies depending on the pitch-to-side ratio. Applying a medium-quality structured mesh resulted in an average error of about 1% over the analyzed parameters, but in no case exceeded 4%, with respect to a fine one. RANS simulations were stopped when the continuity residual fell below $1 \cdot 10^{-5}$ to ensure that each simulation did not exceed 96 hours of computation. For further information regarding the numerical model and the sensitivity analysis, we recommend [8].

3. Results

As mentioned above, the forced convection of air inside the channels analysed takes place at Re 7200. Reynolds number selection is primarily influenced by two factors. Firstly, it represents the upper limit of Reynolds numbers tested thus far with the current experimental setup. Secondly, in line with previous analyses [7], it has been found that the accuracy of the RANS model $k-\omega-$SST improves with increasing Reynolds numbers. Numerical outcomes related to heat transfer properties have been compared with experimental measurements for the selected configurations.

3.1. Bulk temperature and heat exchanged

Before proceeding with the analysis of the thermal characteristics, we would like to have a brief indication of how effectively our numerical model is able to represent the experimental setup. Since at the experimental level the directly measured quantity is the outlet temperature, it is possible to compare it with the bulk temperature obtained numerically at the outlet section T_{out}. The error is very small for each configuration considered as shown in figure 2. A quantity that is more representative of the problem, could be the thermal power Q. The heat exchanged by the whole channel is calculated as Q in equation 1 and the errors remains below 5% for all the channel configurations except P40S4 V_{donw}, figure 3.

$$Q = \dot{m} c_p (T_{out} - T_{in}) \tag{1}$$

Both figures show, in addition to the experimental and numerical values, the associated experimental uncertainties, represented by means of error bars. In particular, the temperature was measured with a accuracy of $0.05K$, while the uncertainty on the heat exchanged was calculated using the Moffat method [9] and is equal to 2.3%.

3.2. Convective heat transfer coefficient (HTC)

Integral results for heat transfer characteristics are expressed by means of the mean convective HTC computed via $\Delta T_{m,ln}$ when a temperature profile can be considered developed inside a channel with an imposed wall temperature. Then, the mean convective HTC $h_{m,ln}$ can be computed from the energy balance as in equation 2.

$$h_{m,ln} = \dot{m} c_p (T_{out} - T_{in}) / (A \Delta T_{m,ln}) \tag{2}$$

The comparison between the experimentally determined mean convective HTC and those calculated numerically, is shown in figure 4. The values obtained by CFD underestimate the experimental ones except for P10S4 for both V_{down} and V_{up}.

The discrepancies can be attributed to factors arising from both the application of the RANS model and the assumption of fully developed temperature profile inside the channels, which may not be achieved. Numerical results are consistent with the experimental findings, with discrepancies remaining below 10% for all the configurations except for P40S4 V_{down} that

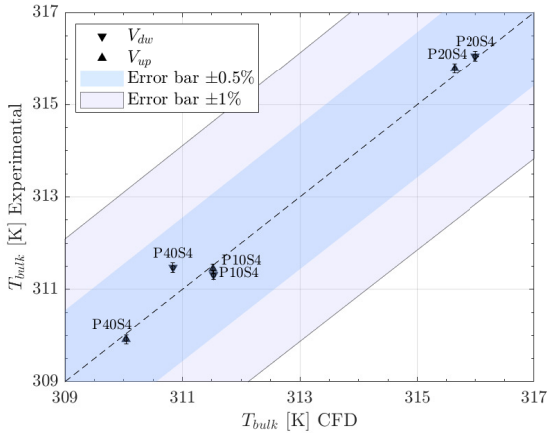

Figure 2. T_{bulk}, comparison between experimental and CFD data.

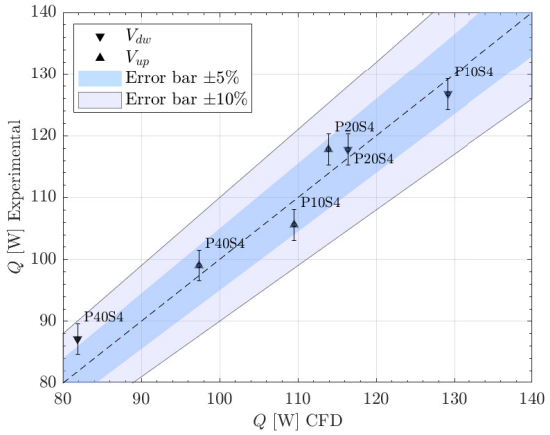

Figure 3. Q, comparison between experimental and CFD data.

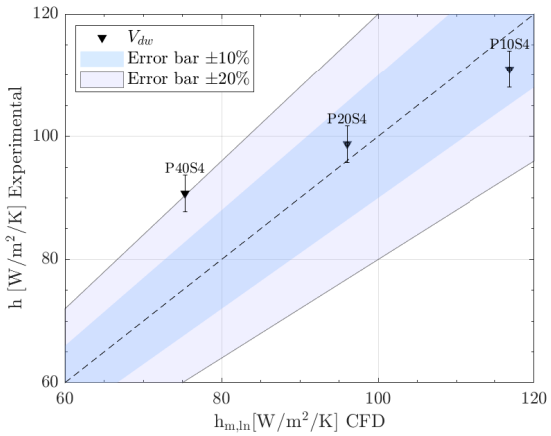

(a) V-down configuration.

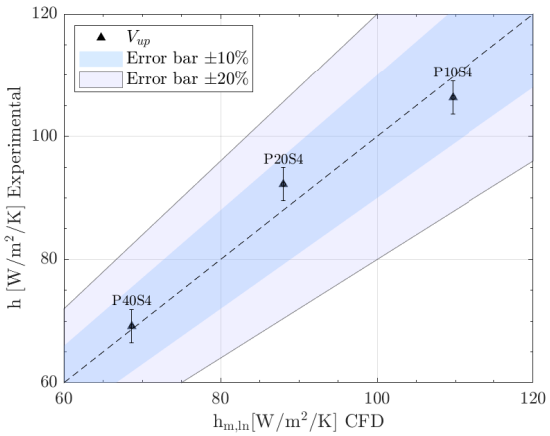

(b) V-up configuration.

Figure 4. $h_{m,ln}$, comparison between experimental and CFD data.

reaches 20%. The capability of the RANS model to capture the associated flow and heat transfer phenomena is quite good. It's worth noting that the uncertainty associated with the experimental convective HTC is 3%.

To see how effective the developed temperature field assumption is, we can investigate the local convective HTC.

The local convective HTC is computed as h_z, equation 3.

$$h_z = q_z/(T_w - T_{b,z}) \tag{3}$$

T_b and the heat flux q_z have been evaluated as mean section variables and mean line variables, in that order, on surfaces and lines built along the channel length, equidistant from each other, and

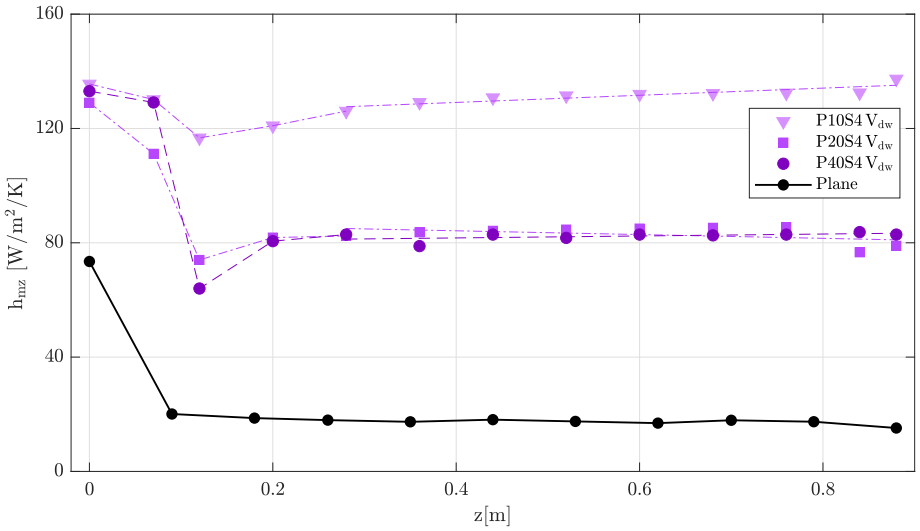

(a) V-down configuration.

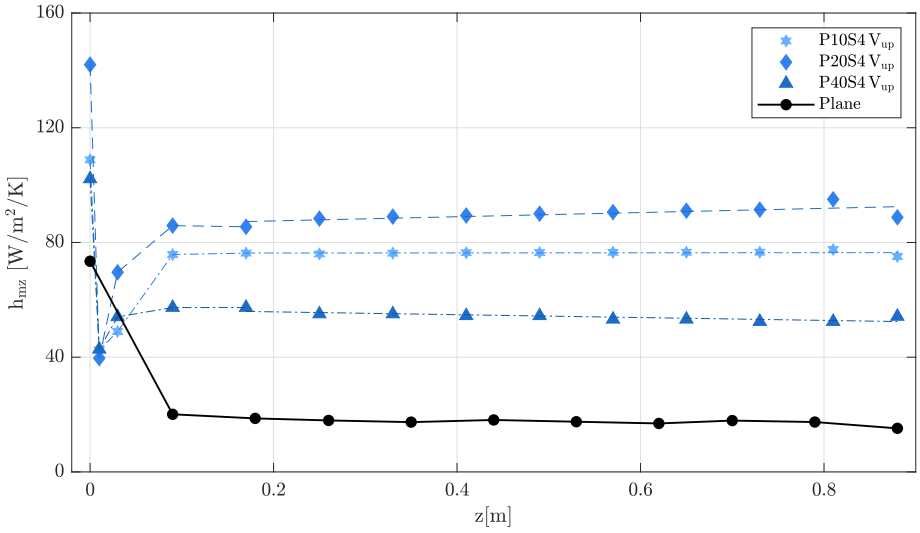

(b) V-up configuration.

Figure 5. Trend of the local convective HTC

in a number that ensures that the convective HTC is no longer affected by their numbers. Then each contribution of the local convective HTC h_z has been weighted through the heat transfer area ΔA_z of influence, and presented in figure 5 as h_{mz}. The figure illustrates the trend of the local convective HTC, h_{mz}, plotted against the channel length, z. Additionally, the distribution of h_z for a plane channel is included for comparison. The presence of the ribs brings a substantial change in the evolution of the local convective HTC, both in terms of the distribution of h_z along z and the value assumed (please note the different values of the y-axis). However, the trends of h_z in the case of ribbed channels present similar pattern, after taking into account the inlet effects the coefficient stabilizes around a value and the distribution becomes almost flat representing a state of thermally developed flow. Only for the V_{down} P10S4 configuration the distributions seem to deviate, probably because this condition is not fully achieved or because the RANS model is not sensitive enough to the complexity of the case.

We want to propose in detail the distribution along the channel length of h_z for the P40S4 V_{up} configuration thanks to figure 6. The local convective heat transfer coefficient increases significantly immediately after the rib until it gradually decreases as the effect of the obstacle decreases. We would also like to point out that after the first two modules, the distribution of h_z between two ribs follows the same shape, i.e. it increases, stabilises, decreases and then increases again, and the values tend to repeat themselves the same at the same distance. In order to increase heat transfer, this shows how tighter ribs are more effective.

At this point it is interesting to propose the actual convective HTC, h_m (equation 4), built considering each contribution of the local convective HTC h_z weighted by the affected heat transfer area ΔA_z. The actual convective HTC offers more exhaustive evaluation compared to $h_{m,ln}$, as it takes into account not only the impact of the channel entrance but also the variations in h_z along the channel.

$$h_m = \frac{1}{\sum_{z=1}^{n_{sections}} \Delta \ A_z} \left(\sum_{z=1}^{n_{sections}} h_z A_z \right) \tag{4}$$

To get an indication of how much the use of $h_{m,ln}$ introduces an error compared to the use of the actual h_m, we propose to compare them in a portion of the channel domain that does not take into account the inlet and outlet effects, starting the evaluation from $z = 0.2m$ until just before the outlet section. Figure 7 shows these data, it can be seen that the error remains

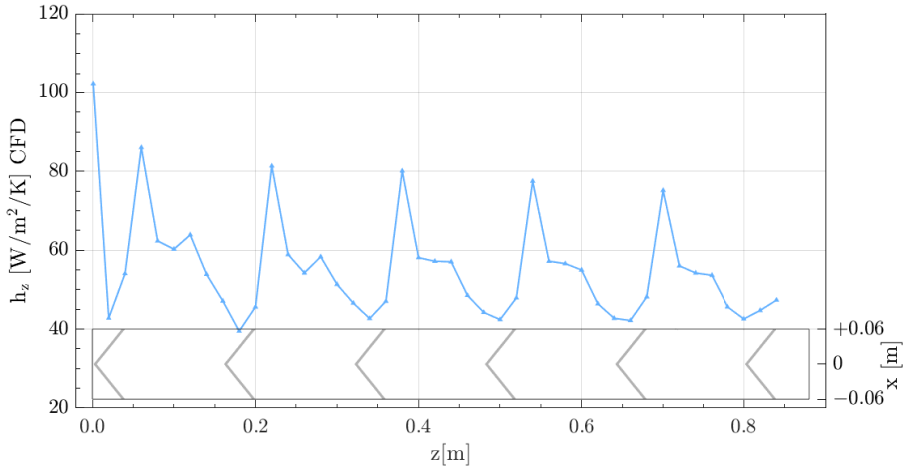

Figure 6. Detailed trend of the local convective HTC h_z for P40S4 V_{up} channel configuration.

always below 20%, the worst behavior is of those configurations that, looking at the trend of h_z in figure 5, show a distribution that is not yet flat but slightly increasing like P10S4 both V_{up} and V_{down}.

4. Discussion and Conclusions

A CFD model for a high aspect ratio rectangular channel with ribs on the upper and lower walls in V-down and V-up configuration has been presented with this work. The RANS $k-\omega-$SST turbulence model has been used, which showed good agreement by comparing the main heat transfer characteristics. Besides, this study confirms literature findings that V_{down} ribs provide better heat transfer enhancement than V_{up}, combined with the fact that it shows us how the closer the ribs are, the greater the increase in heat transfer. Thanks to the results obtained, it is also possible to use this CFD RANS model for different dimensionless pitch-to-side ratios, included in the analyzed range, at an early stage of parametric studies. This work is, actually, a further step of a more comprehensive work. Over time we have built CFD RANS models for different configurations, so that we have managed to have an efficient CFD model for ribs at 90°, 60° tilted and 60° V_{down} and V_{up}, the most popular in the literature. Starting from these CFD models, the idea is to find by an optimization process innovative geometries according to new design methods based on additive manufacturing that can further increase the heat transfer. Performance of these geometries will be first numerically tested by RANS model, in order to select the most promising once that will be further investigated with more accurate CFD simulations - such as LES -, and eventually experimentally. Now that the authors have found that the flow becomes thermally fully developed for most of the geometries analysed, this will allow the use of a periodic domain. Thus, by reducing the domain, we can increase the complexity of the simulation by dealing with the LES approach, for instance.

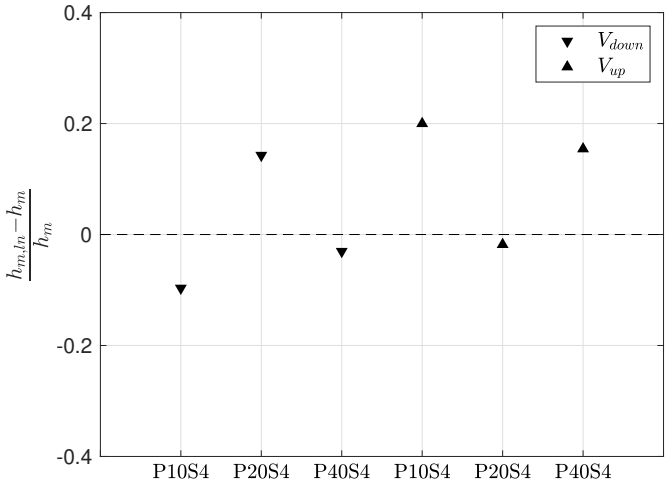

Figure 7. Comparison of convective HTCs computed from CFD results.

Acknowledgments

This work has been partially funded by means of the EU - Next GenerationEU - Project 2022SJP2A5 - CUP D53D23004040006 after the competitive MUR Call n.104 - PRIN 2022.

References

[1] Wang X, Li B, Gerada D, Huang K, Stone I, Worrall S and Yan Y 2022 *Appl. Therm. Eng.* **201** 117758
[2] Sharma S K and Kalamkar V R 2015 *Renew. Sustain. Energy Rev.* **41** 413–435
[3] Alam T and Kim M H 2017 *Renew. Sustain. Energy Rev.* **69** 387–400
[4] Singh I and Singh S 2018 *Renew. Sustain. Energy Rev.* **92** 405–425
[5] Jain S K, Agrawal G D and Misra R 2019 *Heat Mass Transfer* **55** 3369–3412
[6] Fustinoni D, Gramazio P, Colombo L P and Niro A 2014 *Proc. 15th International Heat Transfer Conference*
[7] Corti M, Gramazio P, Fustinoni D, Vitali L and Niro A 2023 *J. Phys.: Conf. Ser.* **2509** 012009
[8] Corti M, Gramazio P, Fustinoni D and Niro A 2024 *J. Phys.: Conf. Ser.* **2685** 012001
[9] Moffat R J 1988 *Describing the uncertainties in experimental results* vol 1 (Experimental Thermal and Fluid Science)